JOURNAL OF CHEMICAL & ENGINEERING DATA

ARTICLE

pubs.acs.org/jced

Comparison of Various Models to Describe the Charge−pH Dependence of Poly(acrylic acid)

Johannes Lützenkirchen,[*,†] Jan van Male,[‡,§] Frans Leermakers,[§] and Staffan Sjöberg[∥]

[†]Institut für Nukleare Entsorgung, Forschungszentrum Karlsruhe, Postfach 3640, 76021 Karlsruhe, Germany

[‡]Culgi B.V., P.O. Box 252, 2300 AG Leiden, The Netherlands

[§]Laboratory of Physical Chemistry and Colloid Science, Wageningen University, P.O. Box 8038, 6700 EK Wageningen, The Netherlands

[∥]Department of Chemistry, Umeå University, 901 87 Umeå, Sweden

Supporting Information

ABSTRACT: The charge of poly(acrylic acid) (PAA) in dilute aqueous solutions depends on pH and ionic strength. We report new experimental data and test various models to describe the deprotonation of PAA in three different NaCl concentrations. A simple surface complexation approach is found to be very successful: the constant capacitance model requires one pK_a value and one capacitance for excellent fits to the data, with both parameters depending on ionic strength. The use of a self-consistent set of diffuse double layer parameters with one pK_a for flat, spherical, and cylindrical geometry does not result in a satisfactory description of the data, and a number of adjustments to that model were tested to improve the fit. The basic Stern model (BSM) was tested with both plate and cylinder geometry. The cylinder geometry along with strong electrolyte binding was found to be superior to a similar approach involving weak electrolyte binding both in terms of goodness of fit and self-consistency of the parameters. The third approach, the non-ideal competitive consistent adsorption-Donnan (NICCA-Donnan) model, involving one functional group, allows an excellent description of the experimental data. Finally, the polyacid chain was modeled using a mechanistically more realistic self-consistent field (SCF) approach, which allows for radially inhomogeneous distributions of the charges and radial variations in the polymer density and electrostatic potential, while the functional groups can be in protonated, deprotonated, or complexed states. One functional group was insufficient for a satisfactory description of the data. With two segments (one monoprotic, the other diprotic) a reasonable description of the data, including the ionic strength dependence, is achieved, and the tendency of the size of the macro-ion with pH and ionic strength is as expected. This model has the fewest adjustable parameters and is considered the most realistic and comprehensive among the models tested.

INTRODUCTION

The present paper is part of a larger program that attempts to quantify and understand the interaction of poly(acrylic acid) (PAA) with an aluminum oxyhydroxide (boehmite). Understanding of the multicomponent system requires quantification and understanding of the related subsystems. Here we report results for the PAA-hydrogen ion system. Numerous attempts have been published to describe and understand the dissociation of weak polyacids. Thus in an extensive study the group of Prausnitz[1] has evaluated the charging of lysozyme as well as a number of amino acids, and they report the respective pK_a values. The types of modeling for such charging data vary widely,[2−5] and there is some discussion about the meaning of the related pK_a values.[6] We test a number of different models, simple and more advanced, to titration data of PAA. The simple models are widely applied in the context of mineral surfaces and natural organic matter and are capable of describing macroscopic titration data, while more complex models[1−5,7,8] account for additional patterns such as changes in conformation or size.

The description of acid−base data of minerals and adsorption of metals or ligands to minerals are often treated in terms of surface complexation models (SCMs), involving surface chemical equilibria and accounting for the variable surface charge of the mineral. This approach is connected with Schindler[9,10] and Stumm[11] and their respective co-workers but probably originates from prior studies on polyacids. Natural polyelectrolytes (humic substances) have also been treated by SCMs.[12] Despite the success in describing the macroscopic data, the physicochemical nature of macromolecules is more complex than the model concept. Thus, the structure of humic substances is not yet completely understood: the kind and amount of the different functional groups in such molecules is in most cases unknown or associated with a high degree of uncertainty. Therefore, experimental data on synthetic macromolecules, where this information is available, allow us to test models and to compare them. In this paper several SCMs and a humic substance model are compared to an approach that treats the polyelectrolyte as a flexible macromolecule of segments with multiple states (neutral, charged, complexed), and that unlike the others can account for

Special Issue: John M. Prausnitz Festschrift

Received: November 20, 2010
Accepted: February 23, 2011
Published: March 15, 2011

the pH- and ionic strength-dependent polyelectrolyte conformations in a self-consistent way.

Polymer and polyelectrolyte adsorption are covered by a wide conceptual range including the self-consistent field (SCF) theory of Scheutjens and Fleer[13] or the approach proposed by Prausnitz and co-workers.[14] An extension of the SCF theory was applied to natural organic matter adsorption on relatively insoluble hematite.[15] Compared to that system, the boehmite−PAA system involves aqueous solution reactions between dissolved aluminum and PAA, and many of the above cited approaches are not conceptually able to describe expected phenomena such as multidentate coordination of aluminum ions with different carboxylate groups of one PAA or different PAA entities. The aim is to define a range of acid−base models to serve as submodels for the interaction of PAA with dissolved aluminum ions and with mineral surfaces.

The structure of the paper is as follows. The theoretical basis of the different approaches is shortly described. The experimental procedures are given along with a short survey of the calculational aspects. The data are presented, and in the application the models are described and discussed.

THEORETICAL BASIS

Surface Complexation Models. SCMs require the definition of functional groups (in terms of quantity and reactivity) and some electrostatic correction terms in the overall equilibrium constant for a given chemical reaction. For acid−base data, the reactions with the functional groups are usually restricted to hydrogen ions and for some models include the background electrolyte ions.

For PAA the simplest approach considers the deprotonation of the carboxylate entity:

$$-(CH_2-C\{H(COOH)\}-)_i = -(CH_2-C\{H(COO^-)\}-)_i + H^+{}_m \quad (1)$$

$H^+{}_m$ is a hydrogen ion close to the macromolecule, and $-(CH_2-CH-COOH)_i$ is segment i of the PAA chain. The following mass law equation can be written

$$K = [-(CH_2-C\{H(COO^-)\}-)_i]h_m\,[-(CH_2-C\{H(COOH)\}-)_i]^{-1} \quad (2)$$

where [J] is the molal concentration of species J, and h is the hydrogen ion concentration. The deprotonation of the carboxylate groups yields a negative charge on the macromolecule, and therefore further deprotonation from (neighboring) segments is hindered by attractive interactions. SCMs account for this electrostatic effect via an exponential term, which "corrects" h_m with respect to the measurable hydrogen ion concentration in the electroneutral bulk solution, that is, h.

$$h_m = h\exp\{-F\Psi_m/(RT)\} \quad (3)$$

Here, F, R, and T have their usual meaning, and Ψ_m is the electrostatic potential of the polyelectrolyte experienced at the respective location (here at the location of the functional groups). The absolute charge of the polyelectrolyte can be obtained from potentiometric titrations, if the zero level is known. A charge-potential relationship is required to calculate Ψ_m from the charge originating from PAA reactions. Various charge-potential relationships exist, and some of them are applied in this paper.

The Constant Capacitance Model (CCM). The CCM assumes a linear relationship between the charge, σ_m, calculated from the concentration of the protonated species (eq 1) and the potential.

$$\sigma_m = C_{CCM}\Psi_m \quad (4)$$

C_{CCM} is the specific capacitance of the interface. This model is supposed to be valid for sufficiently high ionic strength in the case of oxides. However, it can yield an accurate description even for low ionic strength for which it is physically not applicable.[16] The parameters of this model depend on ionic strength. While the formalism in the treatment of oxide minerals would require the specific surface area of the macromolecule, the definition of a mass specific capacitance value avoids this problem. Also note the proportionality between charge and potential in this approach. The CCM was applied to the primary data, as explained later. The description was judged adequate, even if data at the highest ionic strength were not described with the same accuracy as those at the lower ionic strengths.

The Purely Diffuse Layer Model (DLM). The DLM[17] allows for variation of ionic strength and is typically implemented in surface speciation codes with flat-plate geometry using the Gouy−Chapman equation to correct for electrostatic effects. To test the effect of particle shape, spherical and cylindrical geometries of the macromolecule are additionally assumed in the present study. Approximate analytical solutions of the problems for monovalent electrolytes from literature[18] were implemented in a surface speciation code. The equations used are given below for the flat plate (eq 5), a spherical particle of diameter d (eq 6), and a cylindrical particle of diameter d and arbitrary length (eq 7).

$$I_m = 2\sinh(y_m/2) \quad (5)$$

$$I_m = 2\sinh(y_m/2)[1+1/\{A\cosh^2(y_m/4)\}^{1/2}] \quad (6)$$

$$I_m = 2\sinh(y_m/2)[1+\{\beta^{-2}-1\}/\{A\cosh^2(y_m/4)\}^{1/2}] \quad (7)$$

Here, $I_m = \sigma_m F/(RT\varepsilon_o\varepsilon\kappa)$ is the reduced charge density, $y_m = F\Psi_m/(RT)$ is the reduced potential, $A = d/2\kappa$ and $\beta = K_o(A)/K_1(A)$, where K_i is the ith order Bessel-function and κ is the Debye−Hückel parameter. Whereas the use of the CCM may be entirely on a mass specific basis, the DLMs require an input value for specific surface area, since molar concentrations have to be related to surface specific values. This strongly affects the electrostatic terms via eq 3. For oxide minerals the specific surface area is assumed constant and can be independently measured. For macromolecules a "specific surface area" is relevant to the diffuse layer of counterions and expected to vary with ionic strength and pH, due to conformational changes.

A linear increase of specific surface area with decreasing ionic strength was introduced for all plate geometries. The relative numerical weighting or scaling of this constraint was varied in the parameter estimation procedure. Results turned out to be sensitive to this variation. In the case of the spheres and cylinders surface area can be numerically related to particle size parameters.

The Basic Stern Model (BSM). The BSM is a combination of CCM and DLM but includes electrolyte binding, which in addition to eq 2 requires a sodium binding reaction

$$K_{Na} = [-(CH_2-C\{H(COO^-Na^+)\}-)_i]h_m\,[-(CH_2-C\{H(COOH)\}-)_i]^{-1}[Na^+{}_m]^{-1} \quad (2a)$$

dx.doi.org/10.1021/je101253q |J. Chem. Eng. Data 2011, 56, 1602–1612

The association constant can be written as given in eq 2b

$$K_{\text{el.bind}} = [-(CH_2 - C\{H(COO^-Na^+)\} -)_i] \; [-(CH_2 - C\{H(COO^-)\} -)_i]^{-1}[Na^+{}_m]^{-1} \quad (2b)$$

The hydrogen ion is considered in a first electrostatic layer, while the sodium can be either in the first or in a second one (or both). Values for surface area, capacitance value, and at least two equilibrium constants are required. Since the initial BSM tests were very successful, no further attempts were made to improve the fit, by for example allowing for ionic strength dependent surface areas. The BSM was used with a plate and a cylinder geometry. Although the plate geometry is not realistic, a self-consistent set of parameters can be obtained to calculate the dissociation of PAA as a function of pH with common computer codes (strictly speaking the parameters pertain to the NaCl media we use and the molecular weight of our PAA sample).

The cylinder geometry was treated according to eqs 7a and 7b.

$$I_m = 2\sinh(y_m/2)[1 + \{\beta_{BSM}{}^{-2} - 1\}/\{A\cosh^2(y_m/4)\}^{1/2} \quad (7a)$$

where $A = d/2\kappa$, and d is the distance between the center of the cylinder and the on-set of the diffuse layer and $\beta_{BSM} = K_o(A)/K_1(A)$. The inner layer capacitance of the cylinder can be related to that of a flat plate according to Ohshima et al.[18]

$$C_{1,\text{cyl}} = C_{1,\text{plate}}(d_1/a)/\ln(1 + d_1/a) \quad (7b)$$

where a is the cylinder radius and $d_1 = d/2 - a$, that is, the thickness of the inner layer. $C_{1,\text{plate}}$ is the equivalent plate capacitance, which can related to the local dielectric constant, ε_r, in the inner layer

$$C_{1,\text{plate}} = \varepsilon_o\varepsilon_r/d_1 \quad (7c)$$

The local dielectric constant will be used to test self-consistency of the model with respect to electrolyte binding.

The Non-Ideal Competitive Consistent Adsorption-Donnan (NICCA-Donnan) Model. The general equation for adsorption of a species i within the NICCA-Donnan model[19,20] is

$$\Theta_{i,t} = (K_ic_i)^{n_i}/\sum_i (K_ic_i)^{n_i}[\sum_i (K_ic_i)^{n_i}]^p/\{1 + [\sum_i (K_ic_i)^{n_i}]^p\} \quad (8)$$

where $\Theta_{i,t}$ is the fraction of all sites occupied by species i, K_i is the median value of the affinity distribution for species i, c_i is the concentration (or activity) of species i, n_i reflects the overall nonideality, which can be due to lateral and/or stoichiometric effects, and p is the width of the distribution of K_i.

The amount of species i bound, Q_i, is given by

$$Q_i = \Theta_{i,t}Q_{\max}(n_i/n_H) \quad (9)$$

$Q_{\max}$ is the maximum binding capacity. While the model has frequently been applied to natural organic matter usually assuming two sites (carboxylic and phenolic sites), it is possible to involve only one functional group, which for PAA would be expected based on the structure.

The Donnan model is applied for calculating electrostatic correction factors and requires a value for the Donnan volume (V_D) in $dm^3\cdot kg^{-1}$, which is related to ionic strength via the following equation

$$\log V_D = b(1 - \log I) - 1 \quad (10)$$

where b is an empirical fit parameter, and I is the ionic strength in $mol\cdot kg^{-1}$. V_D ranges from (1 to 80) $dm^3\cdot kg^{-1}$ (fulvic acids) and from (0.1 to 5) $dm^3\cdot kg^{-1}$ (humic acids) and b from -0.7 to -0.9 and -0.3 to -0.5, respectively.[19,20] The charge on the macromolecule is assumed to be neutralized by counterions within V_D:

$$q/V_D + \sum_j z_j(c_{Dj} - c_j) = 0 \quad (11)$$

where q is the charge of the macromolecule, c_{Dj} is the Donnan-concentration of j (with charge z_j including sign) and c_j the concentration of j in bulk solution. The two concentrations are related via a Boltzmann factor (f_D)

$$c_{Dj} = c_j f_D{}^{zj} \quad (12)$$

$$f_D = \exp(-\Psi_D F/RT) \quad (13)$$

with the Donnan potential Ψ_D, which is assumed to be distributed over the volume phase, and therefore no assumption about geometry is required.

Several variations were tested, covering the assumption of 1 and 2 sites either with or without specific counterion-binding.

The Self-Consistent Field (SCF) Approach. The SCF approach is targeted to treat one central macromolecule as realistically as possible. In contrast to the NICCA-Donnan model, where the segment density inside the macromolecule and the electrostatic potential are preassumed to be constant and where the system is locally electroneutral, the SCF allows for spatial variations in segment density and electrostatic potential inside the coil. As a result the system is not necessarily locally electroneutral; only the macromolecule with surrounding electrolyte is in total electroneutral. The model is a straightforward extension of the Scheutjens–Fleer model.[13,21] Here we do not go into all details, but we refer to the literature[21] and the Supporting Information. In principle, the SCF approach is able to predict the titration curve as a function of the polymer concentration, but this has not been tested in the present calculations.

A polyelectrolyte was defined in terms of the number of its segments per molecule and the number of molecules in a spherical lattice of known size. Here, one molecule was fixed with its middle segment in the center of a spherical lattice. The lattice was large enough to allow full extension of the molecule without coming close to the reflecting boundary (mirror). The relative permittivity was set to 80, and its value was not changed. All Flory–Huggins parameters were set to zero.

Table 1 gives an overview of the models applied in this study and indicates the numbers and kinds of adjustable parameters involved in the application of those models.

MATERIALS AND METHODS

Experimental Section. Titration data were obtained with PAA from Aldrich (50 % wt. aqueous solution, molecular weight specified by the producer was 5000 D, which was not verified by us). For all solutions boiled Millipore water was used. PAA stock solutions were prepared by diluting a weighed amount of the 50 % wt. solution in a calibrated volumetric flask giving a concentration of about $2\cdot10^{-2}$ $mol\cdot kg^{-1}$ with respect to carboxylate groups. The amount of carboxylate groups in the stock solution was determined from potentiometric titrations, which showed PAA to be fully protonated at $-\log h \leq 2.5$ and fully

Table 1. Overview of the Models Tested and the Respective Overall Numbers of Adjustable Parameters[a]

model	CCM	DLM_{plate}	DLM_{sphere}	$DLM_{cylinder}$	BSM	$BSM_{cylinder}$	NICCA-Donnan	SCF[c]
number of adjustables	6[b]	4 [2]	7 [3]	7 [3]	4	3	5−12	3
adjustables	C	SFA[d] (3)	SFA (3) [1]	SFA (3) [1]	log K	log K		
	log K	[1]	d (3) [1]	d (3)[e] [1]	log $K_{el.bind}$	log $K_{el.bind}$	log K_i	log K
		log K	log K	log K	SFA	C	n_i	
					C			

[a] For the DLM numbers in squared brackets indicate numbers of adjustables for the cases where geometric parameters were assumed to be independent of ionic strength. [b] Two values for each ionic strength. [c] Two segments, no counterion binding. [d] Surface area per mass of polyelectrolyte. [e] Cylinder length fixed, not varied, since no relation between geometry and SFA is assumed (density is unknown).

deprotonated at $-\log h > 9$, where h is the free hydrogen ion concentration. Values were verified by analyzing the total carbon content in the stock solution and in the samples from the titrations. Both methods agreed to within 3 %, and the stock solution concentration was finally set at $2.0863 \cdot 10^{-2}$ mol·kg^{-1}. NaCl dried at 600 K was added to make solutions of the desired ionic strength.

The titrations were carried out on an experimental setup which has previously been described.[22] Titrations were either carried out coulometrically or with dilute standardized NaOH solution containing the respective ionic medium. The NaOH solution was prepared in an argon atmosphere from concentrated NaOH at the minimum of Na_2CO_3 solubility. Titrant solutions were kept in a plastic container with a cushion of argon and never used longer than three weeks. Hydroxyl concentration in this titrant was checked at regular intervals by titration of a solution of known hydrogen ion concentration. Reversibility of the PAA titrations was found in back-titrations using HCl solutions. Titrations were carried out in a thermostatted room (298.15 K ± 0.5 K). The titration vessel was purged with purified and humidified argon. A Ag/AgCl reference electrode was used in combination with a glass electrode. The titration setup is situated in an oil bath at 298.15 K ± 0.05 K. Temperature variations are monitored. The additions of titrants and potential readings are controlled by a computer. Equilibrium was supposed to be achieved when stable potential readings within ± 0.1 mV were recorded. Each titration involved its individual calibration in which a solution of known hydrogen ion concentration was titrated coulometrically or with standardized base solution, so that the parameters in the following equation could be determined

$$E = E_o + 59.16 \log h + E_J \quad (14)$$

E is the measured potential, h is the hydrogen ion concentration, and E_J is the liquid junction potential given by:

$$E_J = j_{ac}h + j_{alk}K_w h^{-1} \quad (15)$$

The parameters j_{ac} and j_{alk} have been determined independently; K_w is the ionic product of water. See Sjöberg et al.[23] for a summary of these parameters. The slope is taken as the ideal (Nernstian) slope, which has been verified independently. E_o is determined from the calibration data.

After the calibration is accomplished a known volume of the PAA stock solution is added and the solution acidified to $-\log h \approx 2.5$ by adding a known volume of a solution containing a known concentration of hydrogen ions. Then the titration of PAA is started using either a coulometer or NaOH solution (titration curves were found to coincide).

Treatment of Experimental Data. Based on the calibration parameters, hydrogen ion consumption functions (here equivalent to the degree of dissociation or deprotonation of PAA, denoted Z_{pol}) are calculated from the measured E values using eqs 14 and 15 according to the following relation

$$Z_{pol} = [H - (h - K_w h^{-1})]/TOTCx \quad (16)$$

In eq 16, the symbols have the following meanings:

- H — total (analytical) concentration of hydrogen ions calculated over a zero level defined by the fully protonated PAA, implying that Z_{pol} attains values between 0 and −1 (c.f. Figure 1); $|Z_{pol}|$ corresponds to the degree of dissociation α, often used in the polyelectrolyte literature
- h — free concentration of hydrogen ions calculated from the measured E and the calibration parameters
- TOTCx — total (analytical) concentration of carboxylate groups

In titrations with NaOH solutions the dilution of the system is taken into account. The coulometric titrations have the advantage that no dilution occurs. It was found that experimental Z_{pol} versus $-\log h$ curves agree very well for all concentration ranges studied for both ways of increasing the pH. Data are presented on the concentration scale, that is, as $-\log h$.

Technical Details on Calculations. In the first step CCM parameters were fitted to each individual experimental data set. From the CCM calculations the hydrogen ion consumption functions were calculated using the respective parameters obtained with the individual data sets at fixed $-\log h$ intervals. A mean value for each ionic strength was thus obtained. Experimental errors were also calculated from the individual CCM models on the basis of hydrogen ion consumption functions. All calculations (except those involving the CCM, where raw data were treated) were done on hydrogen ion consumption functions, that is, normalized titration data. These hydrogen ion consumption functions were calculated from the mean CCM parameters and corrected for effects of dilution and total concentrations. The advantage of this procedure is that the weighting of data points in the inverse modeling is realistic and comparable goodness of fit parameters are obtained.

The inverse modeling for the CCM was done using UCODE[24] in combination with FITEQL3.1.[25] FITEQL is a data fitting code but can be used as a pure speciation code, that is, as an application called by UCODE.

Other codes used were modified versions of FITEQL2.0[26] as well as FIT[27] and ECOSAT.[28] More details on the procedures can be found in the Supporting Information.

For the SCF calculations, the final concentration of the macromolecules in the experiments was sufficiently low to ignore

Table 2. Averaged Parameters for the CCM Description of the PAA Data (Figure 1)[a]

I	C	
mol·kg^{-1}	F·g^{-1}	log K
0.05	0.73 ± 0.01	−4.56 ± 0.03
0.10	0.91 ± 0.02	−4.43 ± 0.04
0.60	1.18 ± 0.01	−4.23 ± 0.03
0.00 (linear extrapolation)	0.76 (R^2 = 0.90)	−4.53 (R^2 = 0.90)
0.00 (square root extrapolation)	0.61 (R^2 = 0.94)	−4.65 (R^2 = 0.94)

[a] These values are used to generate mean experimental data for the other model approaches and experimental error estimates. Extrapolation of the two respective parameters to zero ionic strength.

interactions between macromolecules, allowing the use of one macromolecule in the calculations. The size of the lattice sites was based on previous experience. The assignment of a segment to a lattice site started from the simplest configuration possible (i.e., the one given in eq 1) and then gradually made more complex by introducing additional states (including electrolyte binding) and/or by defining different segments. For the model results presented later the size of a segment corresponded to the dimension of a lattice site.

Comparative Evaluation of Goodness of Fit. With the CCM mean parameters at each value of ionic strength, mean error squares were calculated based on the various individual models for each data set at the respective ionic strength for −log h from 2.9 to 8.3 at 17 discrete points according to

$$es_{mod} = \sum(Z_{pol,calc} - Z_{pol,CCM})^2/n_p \qquad (17)$$

with

"calc" calculated values (by SCMs, NICCA-Donnan, or SCF models)

"CCM" calculated with the mean CCM parameters, reference values

n_p the number of data points (n_p = 51, that is, 17 for each ionic strength)

For the sake of comparison the above values which are calculated by the mean CCM parameters can be compared to the individually calculated CCM values (index "pol,ind,CCM")

$$es_{ref} = \sum(Z_{pol,CCM} - Z_{pol,ind,CCM})^2/n_p \qquad (18)$$

In eqs 17 and 18 the sum is over all 51 data points. The reference value es_{ref} was calculated to be $4.4 \cdot 10^{-5}$. The error squares obtained from the model performance should be of the order of the error squares calculated by this last equation for a reasonable fit to the data. Goodness of fit will be given as es_{mod}/es_{ref}. Apart from this goodness of fit criterion, the number of adjustable parameters will be reported.

Table 2 summarizes the parameters obtained within the CCM. The parameters vary with ionic strength, since the application of the CCM is consistent with a constant ionic medium approach. Possible functional correlations of the parameters with ionic strength were checked and are reported in Table 2 as well.

RESULTS AND DISCUSSION

Experimental Results. In Figure 1 the experimental data are shown for all background electrolyte concentrations studied.

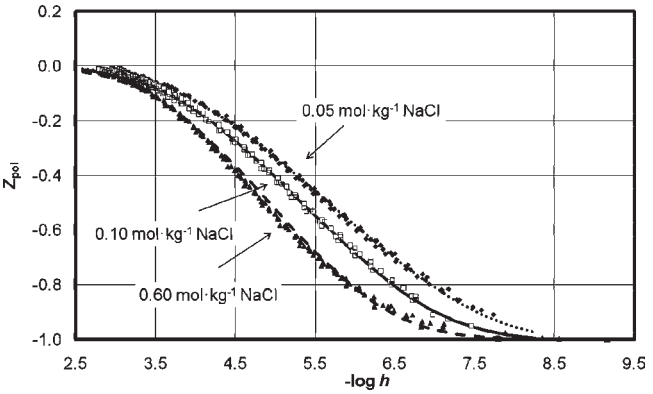

Figure 1. Experimental data and average CCM model performance at different background electrolyte concentrations (see Table 1 for the model parameters) for different NaCl contents. ▲ and dashed line, 0.6 mol·kg^{-1}; □ and full line, 0.1 mol·kg^{-1}; ♦ and dotted line: 0.05 mol·kg^{-1}.

Different symbols indicate separate experiments. The results agree well with previously published data for PAA (see Figure SI1 in Supporting Information). The bold lines are the reference ("averaged") data sets denoted by the index "pol,CCM" in the previous section, which were used in the modeling exercises reported in the subsequent sections. Because of the many different model variations tested, not all modeling results can be plotted. Instead goodness of fit parameters and mean equilibrium constants are reported in the relevant tables.

Modeling. Figure 1 includes the average CCM models. The parameters are summarized in Table 2. With two adjustable parameters for each respective value of ionic strength, it is possible to obtain an accurate description of the data, even if the model itself is rather unrealistic for a flexible polyelectrolyte. The description of the experimental data was slightly worse for the 0.6 mol·kg^{-1} NaCl data as compared to the data collected at lower ionic strengths. It was verified that the description of the data at the highest ionic strength would not influence the results presented below. The overall good fit to the data indicates that this simple model is of a reasonable mathematical form. The next model approach included the DLMs.

As a first step traditional versions of the DLM were applied. For the flat plate geometry a common computer code like FITEQL can be used. As indicated above, in the case of the sphere and cylinder geometries respective analytical approximations[18] were implemented in FITEQL. For these cases besides the specific surface area a diameter for the sphere or the cylinder are required.

In a first attempt the geometric parameters were assumed to be independent of ionic strength to keep the system as simple as possible, although it is expected that they should vary with macromolecule shape and thus with salt content and pH. This explains the poor fit obtained with these first three model variants (Table 3). To improve this, the geometric parameters were in second series of calculations allowed to vary with ionic strength. The outcome of these calculations was that in general a strong dependence of final results on the initial parameters was observed. The initial geometric parameters were varied in such a way that the "surface area" of the polymer would increase with decreasing ionic strength, and the diameter would decrease with ionic

strength. In the range of initial parameter values tested, the results shown in Table 4 were the best fit parameters that could be obtained. For the most unrealistic, that is, flat-plate, geometry no consistent trend in surface area resulted except for one set of initial parameters. Even starting from the optimized parameters of this run, the subsequent optimization would diverge in the sense that the goodness of fit would improve, but the expected trend in the geometric parameters was not obtained. It is obvious that the plate results differ strongly from the more realistic geometries with respect to both the geometric parameters such as model surface area and the equilibrium constant. The results of the sphere and cylinder geometry are relatively close with respect to the model inherent surface area, the diameter, and the equilibrium constant. The goodness of fit is better for the cylinder geometry. Although for the cylinder geometry the goodness of fit relative to the estimated experimental error is among the most successful of all models tested, the model concept involves assumptions that are not expected to hold. Thus the conformational changes would result in changes of the "specific surface area" and the diameter with pH, which the model does not account for. We can estimate the extreme values for the "specific surface area" of PAA for the two idealized geometries. To this end we use parameters summarized by Adamczk et al.[29] For the bare chain diameter (0.71 nm) and the hydrated chain diameter (1.0 nm) along with an extended length for their 12 kD PAA sample we estimate values of (5022 and 7098) $m^2 \cdot g^{-1}$, respectively, which surprisingly is within the range of fitted surface areas. The diameters however are not in agreement with those estimates. Similar estimates for spherical geometries also fail to produce consistent results.

Table 3. Summary of the Overall Mean Adjustable Parameters for the DLM with Ionic Strength Independent Geometric Parameters and Goodness of Fit

model	DLM_{plate}	DLM_{sphere}	$DLM_{cylinder}$
log K	-4.11 ± 0.05	-4.43 ± 0.05	-4.42 ± 0.04
SFA/$m^2 \cdot g^{-1}$	$1.0 \cdot 10^5$	$9.0 \cdot 10^3$	$8.5 \cdot 10^3$
d/nm	NA	385	118
es_{mod}/es_{ref}	398.89	363.54	356.48

Sphere and cylinder can be taken as extreme geometries for the coil and extended polyelectrolyte chain configuration. However, based on available simulations[29,30] it is obvious that the configuration changes between these two extremes in far more complex ways, including for example pearl necklace formation.[30]

Both the sphere and the cylinder model involve a total of seven adjustable parameters for the conditions covered by the experimental work, and the numerical success of the model is most probably related to this issue. This is corroborated by the fact that the flat plate geometry with fewer adjustable parameters was always less successful than the cylinder and sphere options.

The BSM was tested with the plate and cylinder geometry. The outcome of the numerical optimizations is given in Table 5. The plate version is surprisingly successful in terms of goodness of fit. This is probably a convenient, easy to use model to reproduce experimental data as a function of pH and electrolyte concentration. The cylinder geometry within the BSM, that is, in conjunction with eqs 7a and 7b (applied with fixed values for a and d_1), also turned out to describe the data quite well. A number of different options were used in this case. First a specific surface area pertaining to the bare chain radius based on the parameters reported by Adamzcyk et al.[29] was used (i.e., 5022 $m^2 \cdot g^{-1}$). Using this fixed value two options were again considered, weak and strong electrolyte binding. The results with both options did not vary too much in terms of goodness of fit, but the strong

Table 4. Summary of the Overall Mean Adjustable Parameters for the DLM with Ionic Strength Dependent Geometric Models and Goodness of Fit

model	DLM_{plate}[a]	DLM_{sphere}	$DLM_{cylinder}$
log K	-4.05	-4.52 ± 0.01	-4.46 ± 0.02
SFA (0.05 mol·kg^{-1})/$m^2 \cdot g^{-1}$	$1.0 \cdot 10^4$	$(5.6 \pm 1.8) \cdot 10^3$	$(6.0 \pm 1.3) \cdot 10^3$
SFA (0.1 mol·kg^{-1})/$m^2 \cdot g^{-1}$	$9.8 \cdot 10^3$	$(1.4 \pm 1.0) \cdot 10^3$	$(3.4 \pm 0.9) \cdot 10^3$
SFA (0.6 mol·kg^{-1})/$m^2 \cdot g^{-1}$	$9.1 \cdot 10^3$	$(1.6 \pm 0.8) \cdot 10^2$	$(9.6 \pm 3.1) \cdot 10^2$
d (0.05 mol·kg^{-1})/nm	NA	10.7 ± 6.7	56.7 ± 27.4
d (0.1 mol·kg^{-1})/nm	NA	8.1 ± 6.1	8.9 ± 3.4
d (0.6 mol·kg^{-1})/nm	NA	0.5 ± 0.2	1.2 ± 0.7
es_{mod}/es_{ref}	11.9	9.0	5.0

[a] Among the many initial values and constraint combinations tested only one such combination resulted in the expected tendency for the surface area with ionic strength.

Table 5. Summary of the Overall Mean Adjustable Parameters for the BSM and Goodness of Fit[a]

model	BSM_{plate}	$BSM_{cylinder,1}$	$BSM_{cylinder,2}$	$BSM_{cylinder,3}$	$BSM_{cylinder,4}$	$BSM_{cylinder,5}$
			"Weak" Electrolyte Binding			
log K	-4.16 ± 0.03	-4.30 ± 0.03	-4.37 ± 0.03	-4.40 ± 0.03	-4.40 ± 0.04	-4.33 ± 0.03
log $K_{el.bind}$	-0.06 ± 0.05	-1.79 ± 0.10	-1.77 ± 0.28	-1.20 ± 0.38	-1.30 ± 0.91	-1.73 ± 0.03
SFA/$m^2 \cdot g^{-1}$	$2.12 \cdot 10^2$	$5.022 \cdot 10^3$ (fixed)	$6.000 \cdot 10^3$ (fixed)	$7.098 \cdot 10^3$ (fixed)	$6.950 \cdot 10^3$	$5.022 \cdot 10^3$ (inner); $9.289 \cdot 10^3$ (outer); both fixed
C/F·m^{-2}	21.90 ± 0.00	23.60 (m)	13.80 ± 0.11	5.53 ± 0.18	6.37 ± 0.42	83.4
es_{mod}/es_{ref}	5.39	9.63	7.26	6.88	6.87	8.54
ε_r	735	792	463	185	214	2800
			"Strong" Electrolyte Binding			
log K	-4.19 ± 0.04	-4.41 ± 0.03	-4.48 ± 0.03	-4.47 ± 0.03	-4.52 ± 0.03	-4.39 ± 0.04
log $K_{el.bind}$	0.10 ± 0.07	0.05 ± 2.67	0.05 ± 0.34	0.08 ± 0.27	0.09 ± 0.03	0.03 ± 0.53
SFA/$m^2 \cdot g^{-1}$	$2.39 \cdot 10^0 \pm 0.06$	$5.022 \cdot 10^3$ (fixed)	$6.000 \cdot 10^3$ (fixed)	$7.098 \cdot 10^3$ (fixed)	$7.650 \cdot 10^3$	$5.022 \cdot 10^3$ (inner); $9.289 \cdot 10^3$ (outer); both fixed
C/F·m^{-2}	1.74 ± 0.03	3.30 ± 0.03	2.91 ± 0.02	2.25 ± 0.02	2.24 ± 0.06	3.76 ± 0.05
es_{mod}/es_{ref}	1.72	10.21	7.98	6.70	6.06	17.01
ε_r	58	111	98	76	75	735

[a] (m) fixed manually, that is, adjusted manually until best fit was achieved.

dx.doi.org/10.1021/je101253q |J. Chem. Eng. Data 2011, 56, 1602–1612

Table 6. Parameters Required for the Various Versions of the NICCA-Donnan Model[a]

model	option	number of adjustables	adjustables
ND_1	1 site no explicit Na binding	5	K_H, n_H, b, Q_{max}, Q_0
ND_2	1 site explicit Na binding	7	K_H, n_H, b, Q_{max}, Q_0K_{Na}, n_{Na}

[a] Q_0 is the amount of hydrogen ions initially sorbed, that is, a parameter that adjusts the level in the protonation data.

Table 7. Parameter Values for the NICCA-Donnan Description of the PAA Data

parameter	ND_1	ND_2
$-b(Vd)$	0.34	0.52
log Q_0	1.15	1.15
log Q_{max1}	1.18	1.19
log K_{H1}	4.29	3.51
log n_{H1}	−0.22	−0.26
log K_{Na1}	NA	−1.52
log n_{Na1}	NA	0.49
es_{mod}/es_{ref}	9.36	6.99

electrolyte binding yielded a more reasonable plate-equivalent capacitance value. With strong electrolyte binding the hydrogen ion binding constant decreased as would be expected. The second case considered an intermediate value for the specific surface area (i.e., 6000 $m^2 \cdot g^{-1}$) based on the values given Adamzcyk et al.[29] for bare and hydrated radii. Again weak and strong electrolyte binding was tested and as for the previous case weak binding resulted in a better fit at the expense of an unreasonable value for the capacitance, when recalculated to a local dielectric constant. The third case involved the specific surface area based on the hydrated chain radius, and again the same results were obtained with respect to the tendency between weak and strong electrolyte binding. There is also a trend with increasing specific surface area, higher values resulting in a better fit and producing more "reasonable" values of the capacitance value. Best fit specific surface areas were also obtained as the final case in this series of calculations. For the weak electrolyte binding, this resulted in a marginal gain in goodness of fit, while for the strong electrolyte binding the fit became clearly better at the optimized value of specific surface area.

A last option within the cylinder geometry considered that the two planes of adsorption actually would have two different areas, which is realistic for such small particles with Stern layers. Using this option, as shown in Table 5 (last column), produced much higher goodness of fit parameters, that is, the fit became worse. In this case we considered the bare chain radius for the inner plane surface and for the calculation of the outer plane surface we involved the distance between the inner surface and the location of the center of charge of a sodium ion plus its first hydration shell (i.e., 0.297 nm, a value taken from a simulation[31]), which is the closest approach of a hydrated sodium ion to the bare chain of PAA and this location coincides with the onset of the diffuse layer. Weak electrolyte binding could be best described with a very high capacitance value. Strong electrolyte binding instead resulted in a more reasonable capacitance value.

In eq 7c, the capacitance is related to the local dielectric constant, which can be estimated using the distance between the inner surface and the location of the center of charge of a sodium ion plus its first hydration shell (i.e., 0.297 nm, a value taken from a simulation[31]). This value self-consistently is inherent to all cylinder calculations within the BSM option. High values of the dielectric constant should enhance ion pairing as is evidenced from temperature-dependent studies in aqueous solutions. However, high local dielectric constants and weak electrolyte binding is obtained, which is not consistent. Strong electrolyte binding instead appears more reasonable in that sense with local dielectric constants around the bulk water value or enhanced and relatively strong binding constants. The most realistic case involving two surfaces results in the worst fit in those cases and also produces a very high local dielectric constant associated with the weakest binding constant obtained in that series.

Several options were tested within the NICCA-Donnan concept. Adjustable parameter values and final model performance are summarized in Tables 6 and 7. As a first option a one-site model was tested. Subsequently, a two-site model was also tested. Both of these variants were tested with and without sodium binding. The NICCA-Donnan model involving two sites plus sodium binding on both sites performed best, but in this case the excessive number of parameters caused parameter values that were not considered reasonable. In particular the hydrogen ion release and sodium association constants were highly correlated and in the numerical best fit result these parameters amounted to >10 on the log scale, their difference being relevant for a good fit. Thus only the single site variants of the NICCA-Donnan approach will be further discussed.

Parameters were within reasonable ranges except for selected values in the two-site models. The values of b (eq 10) obtained with all the models are within the range of values found for natural organic matter (9, 10). The results of the model including sodium binding are shown in Figure 2a and the concomitant species distribution for the 0.1 $mol \cdot kg^{-1}$ case in Figure 2b.

The SCF approach was tested starting with a single segment version, then including sodium binding. Subsequently a two-segment option was used, where the selected segments would fit into the size of the grid used in the calculations. Even this option was tested first without and subsequently with sodium binding to the two segments (in deprotonated form).

The monosegment models were not able to reproduce the data. The slope of the Z_{pol} versus $-\log h$ curves were much steeper than the experimental data. This indicates that the "electrostatic correction to the chemical equilibrium reaction" within this model option and the chosen parameter set cannot create the required shape of the titration curve. The curve rather resembles that of a simple weak acid in solution.

The more successful two-segment approach results in a broader curve via multiple sites and multiple protonation equilibria on one of these sites. The use of two segments corresponding to segment a with the composition $-(CH_2-C\{[COOH]H\}-CH_2)_i-$ and segment b with the composition $-C\{[COOH]H\}-CH_2C\{[COOH]H\}_i-$ therefore resulted in better fits. This discretization of the polyelectrolyte chain results in three deprotonation reactions with three stability constants, one for segment a

$$-(CH_2-C\{[COOH]H\}-CH_2)_i = -(CH_2-C\{[COO^-]H\}-CH_2)_i + H^+_m \quad (19)$$

and two for segment b

$$-C\{[COOH]H\}-CH_2-C\{[COOH]H\}_i = -C\{[COO^-]H\}-CH_2-C\{[COOH]H\}_i + H^+_m \quad (20)$$

$$-C\{[COOH]H\}-CH_2-C\{[COOH]H\}_i = -C\{[COO^-]H\}-CH_2-C\{[COO^-]H\}_i + 2H^+_m \quad (21)$$

The stability constants optimized for these segments can be related to comparable solution monomers like isobutyric acid

(eq 19) for segment a and dicarboxylic acids for segment b. Such a comparison can be found in Table 8. While the value for segment "a" is quite close to a comparable solution monomer, the parameters for segment "b" diverge relatively strongly from the range of stability constants published for the segment analogue.

The final model results corresponding to the two-segment option without sodium binding are shown in Figure 3a for the best fit model obtained.

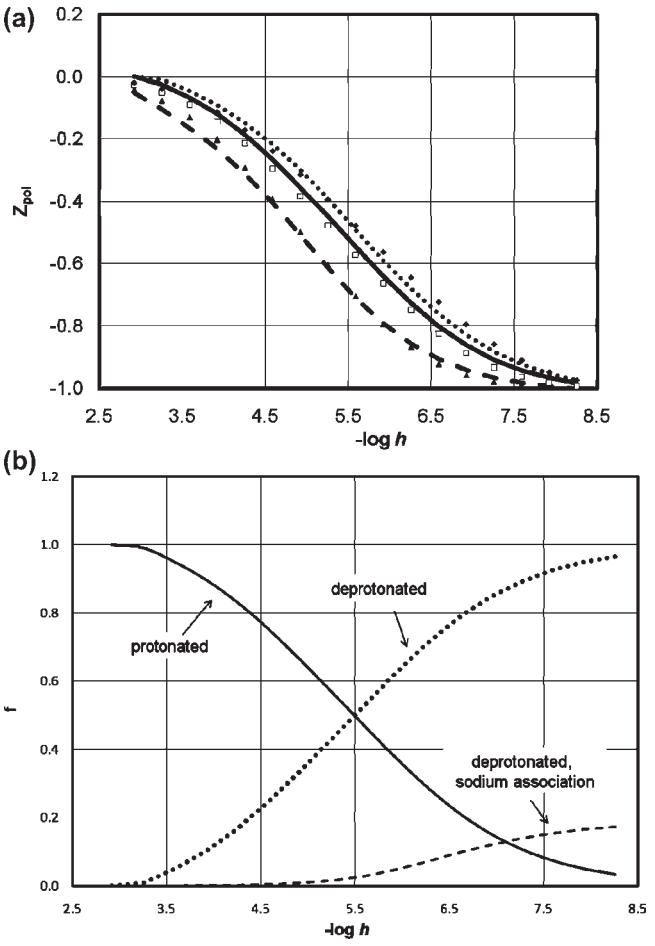

Figure 2. (a) NICCA-Donnan model performance (including sodium, Table 7) in terms of Z_{pol} as a function of $-\log h$ for different NaCl contents. ▲ and dashed line, 0.6 mol·kg^{-1}; □ and full line, 0.1 mol·kg^{-1}; ♦ and dotted line, 0.05 mol·kg^{-1}. (b) Species distribution in terms of fraction, *f*, as a function of $-\log h$ for the 0.1 mol·kg^{-1} NaCl case according to the NICCA-Donnan model. The full line shows the contribution from the protonated species, dotted line from the deprotonated species, and dashed line shows the model inherent contribution of the sodium association to the overall deprotonation.

The numerical fit to the data is not as good as with the other models, but overall only three adjustable parameters were used in this option. The fitting procedure was expected to be rather difficult since two of the deprotonation constants of the two segments have exactly the same hydrogen ion stoichiometry. Therefore, the constant for segment "a" was adjusted manually in the optimization runs, and only the remaining two were adjusted. The manual variation of the former was carried out to obtain a minimum of the goodness of fit parameter.

When sodium association was considered, a common association constant was used for all deprotonated sites, but interestingly including the sodium association did not improve the fit. Sodium association would in all cases tend to increase the degree of dissociation, but without the explicit sodium binding the trends in the medium to high pH range studied is such that the addition of sodium binding would improve only one of three curves. In that pH range sodium association would be most relevant based on competition with hydrogen ions (low hydrogen ion concentration).

From among all models tested the SCF model was estimated to be the most realistic one; the conclusion would be that sodium association in terms of species formation is improbable. This, however, is in conflict with the widely accepted affinity of the sodium ion with carboxylate groups.[32]

The nature of the interaction between sodium and one of the simplest carboxylate groups, namely acetate, appears rather complex.[33] Combined spectroscopic and potentiometric investigation on the interaction of sodium with acetate suggest the presence of both inner-sphere and outer-sphere complexes in solutions.[33] Stability constants (log scale) for the association reactions (i.e., the reaction between acetate and sodium, equivalent to our notation) at 293.15 K, reduced to zero ionic strength, were reported to be 1.14 and 0.24 for inner- and outersphere association, respectively. This duality in binding modes may be responsible for the good fits with both strong and weak electrolyte binding on PAA. No attempt was made to involve both modes in the BSM options, because potentiometric data usually do not allow the distinction between the two modes.[33]

Calculations with the SCF approach yield results for the geometric extension of the polyelectrolyte as a function of pH and ionic strength as shown in Figure 3b. The results agree with the expected trends; that is, the effect of increasing charge on the polyelectrolyte causes a stretching of the molecule, which is more pronounced in solutions with lower NaCl concentrations, since the shielding of the charges on the PAA chain is less effective.

Figure 4 shows a comparison of the deprotonation of the segments on the PAA molecule in comparison with the relevant entities in solution at 0.05 molar background electrolyte. The results indicate a more or less parallel shift of the curves, primarily caused by electrostatic effects (for segment a) and concomitant action of electrostatics and differences in the stability constants for segment b, where the shift is clearly not entirely parallel.

Table 8. Parameters for the SCF Approach Description of the PAA Data (Figure 3a and b)[a]

compound	log K^b	segment analogue	log K^c	es_{mod}/es_{ref}
2-methylpropanoic acid (isobutyric acid)	−4.849	a	−4.99	16.27
propanedioic acid (malonic acid)	−2.57 to −2.847	b	−3.85	
propanedioic acid (malonic acid)	−5.07 to −5.696	b	−6.36	

[a] First log *K* values are those found in data bases for aqueous solutions. The log *K* for the segment analogues corresponds to those fitted to the experimental polyelectrolyte titration data. [b] Values from Smith and Martell. [c] Values fitted to the model.

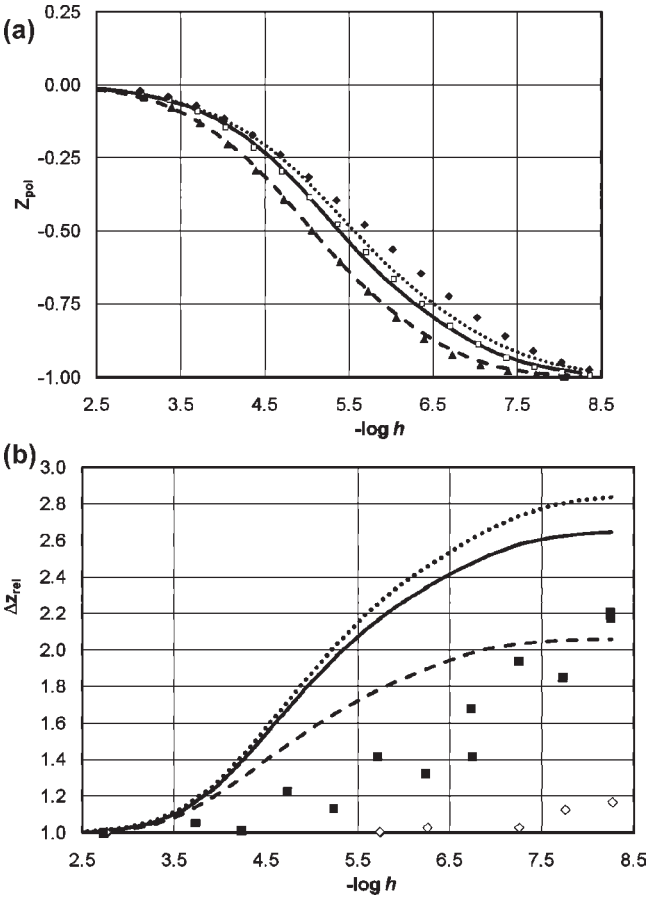

Figure 3. (a) SCF approach model performance (two segments, no sodium association, see Table 8) in terms of Z_{pol} as a function of $-\log h$ for different NaCl contents: ▲ and dashed line, 0.6 mol·kg^{-1}; □ and full line, 0.1 mol·kg^{-1}; and ♦ and dotted line, 0.05 mol·kg^{-1}. (b) Relative extension of PAA, Δz_{rel}, as a function of $-\log h$: relative end-segment position in lattice as a function of hydrogen ion and salt concentration (lines: dashed line: 0.6 mol·kg^{-1}, full line: 0.1 mol·kg^{-1}, dotted line: 0.05 mol·kg^{-1}). For comparison we show results of Monte Carlo simulations for the radius of gyration by Laguecir et al.[5] obtained for 0.001 mol·kg^{-1} background electrolyte concentrations and for $N = 70$ (◇) and $N = 700$ (■), where N is the number of segments on the polyelectrolyte.

Figure 5 shows the effect of ionic strength on the individual contributions from the two segments on the PAA as obtained from the best fit SCF model. Over much of the pH range it is just a parallel shift along the pH range, again as in the above comparison more pronounced for the isobutyric acid segment (segment a), while for segment b the shift at higher pH deviates from the near parallel shift at low pH.

It is worth discussing why the simple SCMs are yielding a very good description of the experimental data. This outcome is maybe not so surprising considering that mean-field approximations to polyelectrolytes like PAA are reasonable, because the distance between charge groups are sufficiently large.[4] Therefore, next-neighbor effects are not of importance.

The SCF approach also involves a mean field to account for the electrostatic effects, but based on the parameter variations carried out in the present work this model could not be reduced to the same simple combination of one segment/two states with mean-field electrostatics. It might be necessary to vary other parameters.

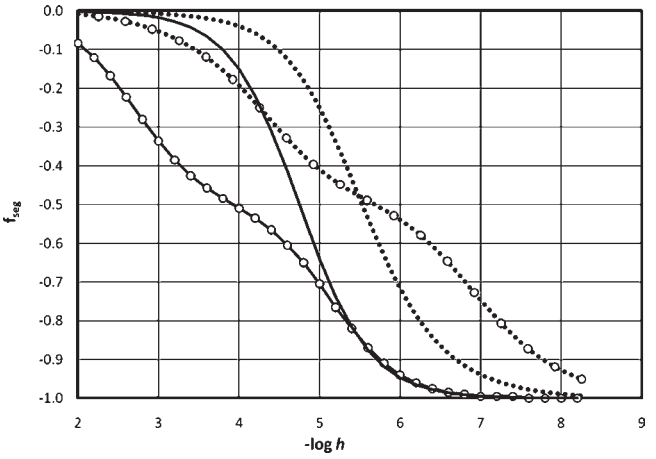

Figure 4. Comparison of the deprotonation patterns (f_{seg}) of the two relevant SCF segments on PAA with the concomitant solution entities, that is, 2-methylpropanoic acid for the monoprotonic segment propanedioic acid for the diprotic segment at $I = 0.05$ mol·kg^{-1}. The dotted lines are for the SCF segments, and the one with the circles (○) refers to the diprotic acid. The full lines are for the solution entities, and again the one with the circles (○) refers to the diprotic acid.

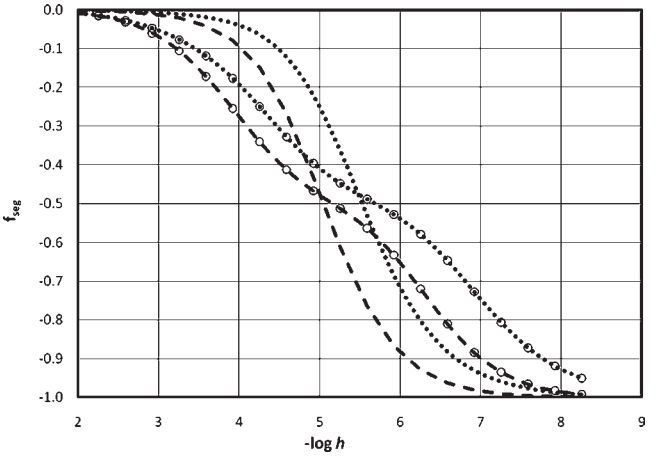

Figure 5. Comparison of the deprotonation patterns of the two relevant SCF segments for the highest and lowest ionic strength investigated. Fraction of deprotonated segment types, f_{seg}, as a function of $-\log h$. 0.6 mol·kg^{-1}: dashed lines without symbol, monoprotic segment; dashed lines with ○, diprotic segment. 0.05 mol·kg^{-1}: dotted lines without symbol, monoprotic segment; dotted lines with ○, diprotic segment.

Such calculations were not pursued, because the SCF approach will not be used in further modeling attempts concerning experimental data on the complexation between dissolved aluminum and PAA. The SCF approach is not capable of handling polydentate complexes which are expected for those systems.

■ SUMMARY AND CONCLUSIONS

In summary it was found that a number of models allow a satisfactory description of the macroscopically observed deprotonation of PAA. Their respective performance can be related to their inherent model assumptions and to the number of adjustable parameters involved. The SCMs do not include pH (and in some

cases ionic strength) related conformations of the macromolecules. The SCF results in Figure 3b suggest that over a wide pH range the effects of pH are much more important than the effects of ionic strength. The NICCA-Donnan models account for effects of ionic strength via the Donnan volumes, but not for the effect of pH on conformation. Consequently, the SCF approach is expected to be the most realistic model. However, the stability constants fitted to one of the segments used in the best fit SCF model did not agree with comparable stability constants for segment analogues, and inclusion of sodium binding did not improve the fit. Figure 3b also includes some results from Monte Carlo simulations on the radius of gyration of PAA as a function of pH at a lower, that is, $1 \cdot 10^{-3}$ mol·kg^{-1}, electrolyte concentration for two different sizes of the polyelectrolyte.[5] The tendency is similar to that obtained from the SCF modeling, but size changes occur at a more acidic pH, and the relative change in size appears to be weaker.

In terms of the number of adjustable parameters within one model variant, the expected tendency to improve the fit to the data by increasing the number of adjustable is retrieved.

When different geometries are compared, DLM cases suggest that cylinder geometry performs best, followed by the sphere geometry. Flat plate geometry is most unrealistic and yields the poorest fit. BSM electrostatics involving plate and cylinder geometry were also tested and found to be successful, but here plate geometry was found to yield better numerical fits. Based on the overall self-consistency of the parameters, a cylinder geometry involving strong electrolyte binding is preferable. Weak electrolyte binding was found to be similar in terms of goodness of fit, but the parameters were not consistent since high local dielectric constants were obtained. In the best performing NICCA-Donnan model, a series of parameters are outside the range of reasonable values, suggesting that this model with up to 12 adjustable parameters is overparameterized. The one site option including sodium binding yields a very good fit to the data (seven parameters).

In conclusion, several models were tested to describe the acid−base properties of PAA. Models ranged from little to highly realistic concerning their representation of the issues affecting the deprotonation of the functional groups.

We note that other models exist to describe titration data of weak polyelectrolyte and refer as one example to the approach suggested by Högeldt et al.[34] These authors applied a three-parameter model to literature PAA titration data. The model requires three pK values for each ionic strength from which a mean pK value is obtained. No attempt is made to include cation binding, which causes a dependence of the average pK value to the trend we obtained for example with the CCM (Table 2). A more recent application of this kind of approach can be found for chitosan samples of different molecular weights.[35] Interestingly, in a very recent paper, Lee and Schlautman[36] have compared the performance of impermeable sphere, Donnan, and cylindrical electrostatic models on acid−base titration curves of linear polyacrylamid-co-acrylate samples. These authors obtained specific surface areas similar to the values estimated in the present paper and concluded that for such samples cylindrical models are more valid and realistic compared to the other models tested. Contrary to our approach Lee and Schlautman[36] fixed a single pK value for all their fittings and had basically the polymer size as an adjustable parameter. Their conclusion that the cylinder geometry better represents the behavior of linear polyelectrolytes is corroborated by our work. Sodium association was not considered by Lee and Schlautman.[36]

It is planned to extend the present work to multicomponent systems, involving dissolved aluminum ions, and to study the adsorption of PAA onto the aluminum oxyhydroxide boehmite. Future plans also include the variations of the PAA molecular weight.

It is to be noted though that not only molecular weight affects the deprotonation of PAA. Kawaguchi and Nagasawa[37] have titrated both isotactic and syndiotactic samples of PAA and found them to be different; see Supporting Information, Figure SI1, which indicates that our experimental raw data in 0.1 mol·kg^{-1} NaCl coincide with the data reported for the isotactic sample reported in the literature in the same ionic medium.[37]

■ ASSOCIATED CONTENT

Supporting Information. Details on the modeling approaches and the codes used as well as the primary titration data. This is further compared to data in literature. This material is available free of charge via the Internet at http://pubs.acs.org.

■ AUTHOR INFORMATION

Corresponding Author
*E-mail address: johannes.luetzenkirchen@kit.edu.

■ REFERENCES

(1) Kuehner, D. E.; Engmann, J.; Fergg, F.; Wernick, M.; Blanch, H. W.; Prausnitz, J. M. Lysozyme Net Charge and Ion Binding in Concentrated Aqueous Electrolyte Solutions. *J. Phys. Chem. B* **1999**, *103*, 1368–1374.

(2) Garces, J. L.; Koper, G. J. M.; Borkovec, M. Ionization equilibria and conformational transitions in polyprotic molecules and polyelectrolytes. *J. Phys. Chem. B* **2006**, *110*, 10937–10950.

(3) Borkovec, M.; Koper, G. J. M.; Piguet, C. Ion binding to polyelectrolytes. *Curr. Opin. Colloid Interface Sci.* **2006**, *11*, 280–289.

(4) Borkovec, M.; Jönsson, B.; Koper, G. J. M. Ionization Processes and Proton Binding in Polyprotic Systems: Small Molecules, Proteins, Interfaces and Polyelectrolytes. *Surf. Colloid Sci.* **2001**, *16*, 99–339.

(5) Laguecir, A.; Ulrich, S.; Labille, J.; Fatin-Rouge, N.; Stoll, S.; Buffle, J. Size and pH effect on electrical and conformational behavior of poly(acrylic acid): Simulation and experiment. *Eur. Polym. J.* **2006**, *42*, 1135–1144.

(6) Ullmann, G. M. Relations between Protonation Constants and Titration Curves in Polyprotic Acids:A Critical View. *J. Phys. Chem. B* **2003**, *107*, 1263–1271.

(7) Leermakers, F. A. M.; Ballauff, M.; Borisov, O. V. Counterion localization in solutions of starlike polyelectrolytes and colloidal polyelectrolyte brushes: A self-consistent theory. *Langmuir* **2008**, *24*, 10026–10034.

(8) Birshtein, T. M.; Mercurieva, A. A.; Leermakers, F. A. M.; Rud, O. V. Conformations of polymer and polyelectrolyte stars. *Polym. Sci. A* **2008**, *50*, 992–1007.

(9) Schindler, P. W.; Gamsjäger, H. Acid-base reactions of the TiO_2 (anatase)−water interface and the point of zero charge of TiO_2 suspensions. *Kolloid-Z. u. Z. Polym.* **1972**, *250*, 759–765.

(10) Schindler, P. W.; Kamber, H. R. Die Acidität von Silanolgruppen. *Helv. Chim. Acta* **1968**, *51*, 1781–1786.

(11) Stumm, W.; Huang, C. P.; Jenkins, S. R. Specific chemical interaction affecting the stability of dispersed systems. *Croat. Chem. Acta* **1970**, *42*, 223–245.

(12) Bolton, K. A.; Sjöberg, S.; Evans, L. J. Proton Binding and Cadmium Complexation Constants for a Soil Humic Acid Using a Quasi-particle Model. *Soil Sci. Soc. Am. J.* **1996**, *60*, 1064–1072.

(13) Scheutjens, J. M. H. M.; Fleer, G. J. Statistical theory of the adsorption of interacting chain molecules. 1. Partition function, segment

density distribution, and adsorption isotherms. *J. Phys. Chem.* **1979**, *83*, 1619–1635.

(14) Beltran, S.; Hooper, H. H.; Blanch, H. W.; Prausnitz, J. M. Monte Carlo Study of Polyelectrolyte Adsorption. Isolated Chains on a Planar Charged Surface. *Macromolecules* **1991**, *24*, 3178–3184.

(15) Vermeer, A. W. P.; Koopal, L. K. Charge Adjustments upon Adsorption of a Weak Polyelectrolyte to a Mineral Oxide: The Hematite−Humic Acid System. *J. Colloid Interface Sci.* **1999**, *212*, 176–185.

(16) Lützenkirchen, J. The constant capacitance model and variable ionic strength: An evaluation of possible applications and applicability. *J. Colloid Interface Sci.* **1999**, *217*, 8–18.

(17) Dzombak, D. A.; Morel, F. M. M. *Surface Complexation Modeling, Hydrous Ferric Oxide*; Wiley: New York, 1990.

(18) Ohshima, H.; Healy, T. W.; White, L. R. Accurate analytic expressions for the surface charge density/surface potential relationship and double-layer potential distribution for a spherical colloidal particle. *J. Colloid Interface Sci.* **1982**, *90*, 17–26.Ohshima, H. Diffuse double layer equations for use in surface complexation models: Approximations and limits. In *Surface complexation modelling*; Lützenkirchen, J., Ed.; Wiley: New York, 2006.

(19) Kinniburgh, D. G.; van Riemsdijk, W. H.; Koopal, L. K.; Benedetti, M. F. Ion binding to humic substances: measurements, models and mechanisms. In *Adsorption of Metals by Geomedia*; Jenne, E. A., Ed.; Elsevier: Amsterdam, 1998; Chapter 23, pp 484−520.

(20) Kinniburgh, D. G.; van Riemsdijk, W. H.; Koopal, L. K.; Borkovec, M.; Benedetti, M. F.; Avena, M. J. Ion binding to natural organic matter: competition, heterogeneity, stoichiometry and thermodynamic consistency. *Colloids Surf., A* **1999**, *151*, 147–166.

(21) van Male, J. Self-consistent-field theory for chain molecules: extensions, computational aspects, and applications. Ph.D. thesis, Wageningen University, The Netherlands, 2003.

(22) Öhman, L. O.; Sjöberg, S. The experimental determination of thermodynamic properties for aqueous aluminium complexes. *Coord. Chem. Rev.* **1996**, *149*, 33–57.

(23) Sjöberg, S.; Hägglund, Y.; Nordin, A.; Ingri, N. Equilibrium and structural studies of silicon(IV) and aluminium(III) in aqueous solution. V. Acidity constants of silicic acid and the ionic product of water in the medium range 0.05−2.0 M Na(Cl) at 25 °C. *Mar. Chem.* **1983**, *13*, 35–44.

(24) Poeter, E. P.; Hill, M. C. UCODE, a computer code for universal inverse modeling. *Computers Geosci.* **1999**, *25*, 457–462.

(25) Herbelin, A. L.; Westall, J. C. *FITEQL: A computer program for determination of chemical equilibrium constants from experimental data*, Version 3.2, Report 96-01; Department of Chemistry, Oregon State University: Corvallis, OR, 1996.

(26) Westall, J. *FITEQL: A Computer Program for Determination of Chemical Equilibrium Constants from Experimental Data*, Version 2.0, Report 82-02; Department of Chemistry, Oregon State University: Corvallis, OR, 1982.

(27) Kinniburgh, D. G. Technical Report WD/93/23: FIT User Guide, *British Geological Survey*, Keyworth, U.K., **1993**.

(28) Keizer, G.; van Riemsdijk, W. H. *ECOSAT: Equilibrium Calculation of Speciation and Transport*, version 4; Wageningen Agricultural University: The Netherlands, 1998.

(29) Adamczyk, Z.; Bratek, A.; Jachimska, B.; Jasinski, T.; Warszynski, P. Structure of Poly(acrylic acid) in Electrolyte solutions determined from Simulations and Viscosity Measurements. *J. Phys. Chem. B* **2006**, *110*, 22426–22435.

(30) Chodanowski, P.; Stoll, S. Monte Carlo simulations of hydrophobic polyelectrolytes: Evidence of complex configurational transitions. *J. Chem. Phys.* **1999**, *111*, 6069–6081.

(31) Mancinelli, R.; Botti, A.; Bruni, F.; Ricci, M. A.; Soper, A. K. Hydration of Sodium, Potassium, and Chloride Ions in Solution and the Concept of Structure Maker/Breaker. *J. Phys. Chem. B* **2007**, *111*, 13570–13577.

(32) Vrbka, L.; Vondrasek, J.; Jagoda-Cwiklik, B.; Vacha, R.; Jungwirth, P. Quantification and rationalization of the higher affinity of sodium over potassium to protein surfaces. *Proc. Natl. Acad. Sci.* **2006**, *103*, 15440–15444.

(33) Fournier, P.; Oelkers, E. H.; Gout, R.; Pokrovski, G. Experimental determination of aqueous sodium-acetate dissociation constants at temperature from 20 to 240 °C. *Chem. Geol.* **1998**, *151*, 69–84.

(34) Högfeldt, E.; Miyajima, T.; Marinsky, J. A.; Muhammed, M. Application of a simple three-parameter model to titration data for some linear polyelectrolytes. *Acta Chem. Scand.* **1989**, *43*, 496–499.

(35) Wang, Q. Z.; Chen, X. G.; Liu, N.; Wang, S. X.; Liu, C. S.; Meng, X. H.; Liu, C. G. Protonation constants of chitosant with different molecular weight and degree of deacetylation. *Carbohyd. Polym.* **2006**, *65*, 194–201.

(36) Lee, B. J.; Schlauman, M. A. Evaluating alternative electrostatic potential models for polyacrylamide-co-acrylate in aqueous solution. *J. Colloid Interface Sci.* **2011**, *354*, 709–717.

(37) Kawaguchi, Y.; Nagasawa, M. Potentiometric titration of stereoregular polyacrylic acids. *J. Phys. Chem.* **1969**, *73*, 4382–4384.